JOURNAL OF ENGINEERING AND EARTH SCIENCES

JEES ISSN: 1897-8680

JEES 2021

VOLUME 14 ISSUE NO 1

PAGE 12-19

INVESTIGATING CORROSION BEHAVIOUR OF COPPER ALLOYED GREY CAST IRON IN ACID AND SALT ENVIRONMENTS

[1]Kutelu, B. J., & [2]Adubi, E. G.

[1]Department of Mineral and Petroleum Resources Engineering, Federal Polytechnic Ado-Ekiti. Ekiti State

[2] Department of Mechanical Engineering, Federal Polytechnic Ado-Ekiti. Ekiti State

Corresponding author email: rinwa2006@yahoo.com

ABSTRACT

Alloying is one of the approaches used for enhancing the service life of grey cast iron in corrosive environments. In this study, four cylindrical cast iron samples were produced in sand mould with constant FeSi–based inoculant (78% Si, 0.21% Al, Fe-bal.) using an in-stream inoculation technique. The first casting was inoculated without copper addition (unalloyed). The second, third and fourth were inoculated with copper additions (alloyed) at 1.4 wt. %, 1.8 wt. % and 2.2 wt. % respectively. The unalloyed casting solidified within slightly hypereutectic range with carbon equivalent (CE) of 4.391. While the 1.4 wt. % Cu, 1.8 wt. % Cu, and 2.21.8 wt. % Cu alloyed castings solidified within hypoeutectic range with carbon equivalent (CE) of 3.940, 3.600, and 4.200 respectively. The microstructure of the unalloyed casting is comprised of spatially dispersed elongated graphite flakes in pearlite matrix. Microstructures of the alloyed castings are comprised of different graphite morphologies in multiphase matrix of ferrite-pearlite. The same trend of corrosion susceptibility was exhibited by the unalloyed and alloyed castings in 0.5 M HCl and 0.5M NaCl solutions. However, the alloyed samples exhibited superior corrosion resistance relative to unalloyed sample. The highest and lowest corrosion behavior in 0.5 M HCl and 0.5M NaCl solutions was shown by the 1.8wt. %Cu alloyed and 2.2wt. %Cu alloyed samples respectively.

KEYWORDS: Alloying elements; Graphite morphologies; Graphitization; Ferrite-Pearlite; Innoculant; Microstructure

INTRODUCTION

Grey cast iron (GCI) is a high carbon ferrous material. The carbon is dispersed through-out the metal matrix and it occurs in the form of a continuous network of graphite flake platelets in pearlitic matrix, or graphite flakes and areas of pearlite in a ferritic matrix (Collini et al., 2008; Sherrif et al., 2019). There are different graphite shapes for flake graphite according to ASTM A 247. Type A graphite is found in inoculated irons cooled at moderate rates, and it is associated with the best mechanical properties. Cast irons with this type of graphite exhibit moderate undercooling during solidification. Type B graphite is found in irons of near-eutectic composition, solidifying on a limited number of nuclei. Large eutectic cell size and low undercooling are common in cast irons exhibiting this type of graphite. Type C graphite occurs in hypereutectic irons as a result of solidification with minimum undercooling. Type D graphite is found in hypoeutectic or eutectic irons solidified at rather high cooling rates and type E graphite is characterized for strongly hypoeutectic irons (Ujiro et al., 1994). The amount of graphite and size, morphology and distribution of graphite lamellas are critical in determining the mechanical behaviour of grey cast iron (Collini et al., 2008; Hammood et al., 2012; Pluphrach, 2010). GCI is used in a wide area of industrial applications due to its good castability, wear resistance, machinability, high damping capacity, and low cost (20–40%

less than steel) (Agunsoye et al., 2014). GCI is characterized by low rate of thermal expansion, good stiffness, resistance to thermal fatigue, good antifriction properties, 100% recyclability and its resistance to compressive stresses 3-4 times of resistance to tensile stresses and good thermal conductivity (Riposan et al., 2012; Seidu, 2014). In industrial practice, an as-cast structure is heterogeneous and characterized by different amounts of carbides, graphite morphologies and variable pearlite/ferrite ratios (Riposan et al., 2012).

Corrosion failure of grey cast iron in aggressive environments has been found to be aided by its brittleness (Riposan et al., 2012; Stan et al., 2010). Lunarska (1996) has attributed corrosion failure of grey cast iron in phosphoric acid solution to cracks that developed at the sharp edges of the graphite particles (Makar & Tromans, 1995). Mohebbi and Li (2011) has shown that localized corrosion was the primary form of corrosion of cast iron water pipes and Krivosheev et al., (1973) revealed that corrosion behavior of cast iron was influenced by additives. Also, promotion of Type A graphite and prevention of undercooled graphite and rosette graphite formation have been achieved through additives (Agunsoye et al., 2014). Consequently, in this study influence of copper additions on the microstructure and corrosion behaviour of grey cast iron in acid and salt environment were investigated.

MATERIALS AND METHOD

Materials

The GCI scraps, inoculant (ferrosilicon), copper wires used for the production of the grey cast irons were sourced from the vendors. The chemical composition of the GCI is shown in Table 1. Other materials are polishing powder, water, grinding papers, polishing cloth, cotton wool, nitric acid and ethanol.

Method

A number of sand moulds were prepared from a mixture of dried fresh silica sand, bentonite, water and coal dust using a cylindrical bar metallic pattern of 190.5 mm long and 18 mm diameter Allowances were allowed for shrinkage, machining, draft, wrapping, and distortion. To allow for an effective and uniform melting rate, the melting furnace (rotary) was preheated for 60-75 minutes. The charged materials including 50kg cast iron auto scraps, 2kg graphite and 1kg limestone were charged into the furnace.

The temperature of the furnace was monitored at regular interval using optical pyrometer. A 60kg ladle was preheated to reduce temperature loss from molten metal during pouring into moulds, and the molten metal was tapped into it at a temperature of 1485^{o}C. The Fe-Si alloy inoculants, comprising of 78% Si, 0.21% Al, Fe-bal with particle sizes in the range 0.5 to 1.5 mm was added directly in the stream The first melt tapped, which is the unalloyed sample serves as the control. The second, third and fourth tapped melts were copper alloyed with 1.4%wt, 1.8%wt and 2.2%wt copper correspondingly. Chemical compositions of the unalloyed and alloyed samples (Table 2) were obtained by Optical Emission Spectroscopy testing machine (ARL QuantoDesk Spectro Analysis Machine).

Microstructure analysis

Machined samples with compositions 0.0%wt. Cu, 1.4%wt. Cu, 1.8%wt. Cu, 2.2%wt. Cu and control were used for the Scanning Electron Microscope examination. The rough surface of the cut sampled was filed to give them a flat surface. The filed surfaces are then ground using laboratory grinding machine with different sets of emery papers starting from the coarsest to the finest and changing the orientation of the sample during each round of ground. Emery papers of 60, 120, 240, 320, 400, 800 and 1200 grits were used. As the emery papers were changed from one to the other, the samples were turned through an angle of 90^{o} so as to remove the scratches sustained from the

previous grinding until a scratch-free surface is obtained Afterward, the samples were polished using a laboratory polishing machine to give a mirror-like surface using billiard cloth and washed with running water, cleaned with alcohol, dried in a warm air in preparation for microscopic examination. The samples were examined under a scanning electron microscope at magnifications of 1000x.

Corrosion studies

The dimensions of the samples (unalloyed and alloyed) for the potentiodynamic polarization test were measured to a precision of ± 0.0l mm with a micrometer screw gauge. They were cold mounted with polymeric material (Epoxy resin) and connected with a flexible wire, ground, polished, cleaned and rinsed properly. AUTOLAB PGSTAT 204N instrument was used for the electrochemical experiments, and it was driven by NOVA software. The experiments were carried out in accordance with ASTM G3-14 (American Society for Testing and Materials G314, 2014) at room temperature. A three-electrode corrosion cell setup, which is comprised of the grey cast iron samples as a working electrode, platinum as counter electrode and silver/ silver chloride as reference electrode was used. Potentiodynamic polarization measurements were carried out at a scan rate of 1.0 mV/s at a potential initiated at −250 to +250 mV. After each experiment, the electrolyte and the test sample were replaced. In this study, all corrosion potential measurements recorded were done respect to the silver/ silver chloride electrode.

RESULTS AND DISCUSSION

Chemical analysis

The results of the chemical analysis of the iron scrap sample in Table 1, showing 2.757 wt. %C, 92.300 wt. %Fe and 1.803 wt. % Si as its major elements and 0.610wt. Cu, 0.0310 wt. % Si, 0.0600 wt. %Mn, 0.738 wt. %Al, 0.0.40 wt. % Mo and 0.1000wt.% P is indicative that the iron scrap sample is GCI (Adedayo, 2013; Lunarska, 1996). Table 2 shows the chemical analysis of the experimentally produced irons. From the results, the contents of carbon, silicon and manganese are in the ranges of 3.01 – 3.10 %, 2.98–2.45 % and 0.234–0.101% respectively. The other residual elements, including P, S and Al are kept at negligible level. The structure of GCI has been shown to depend on chemical composition before the casting process, and cooling conditions (Hammood et al., 2012; Pluphrach, 2010). It is generally well known that graphite formation is favored at high silicon level and carbides at low silicon level (ASTM A247. 2006; Davis, 1996). Consequently, the silicon content (2.45wt. %) of the unalloyed sample, and the silicon content (2.98wt. %) of the alloyed samples at 1.4 wt. % Cu, 1.8 wt. % Cu and 2.2 wt. %Cu are indications that the produced castings are grey cast irons. Silicon and aluminium are known to increase the graphitization potential and number of graphite particles for eutectic and eutectoid transformations, while nickel and copper are known to increase the graphitization potential during the eutectic transformation (ASTM A247. 2006; Krause, 1969). Therefore, the presence of these elements at beneficial level ranges in the castings have further confirmed that the produced samples are GCI. From the evaluated carbon equivalent weight percent (CE wt. %) values in Table 2, it can be seen that the CE value for the unalloyed sample, which is 3.15wt. % is within the hypoeutectic range, and the CE values for the alloyed samples at 1.4wtCu. %, 1.8wtCu. % and 2.2wtCu. %, which are 3.08wt. %, 3.17wt. % and 3.10 wt. % respectively are also within the hypoeutectic range. Hence, the produced samples (alloyed and unalloyed) are hypoeutectic grey cast irons. From Figure 1, it is obvious that CE value was decreased with increased addition of copper and increased with subsequent increase in copper addition. Hence, CE of the produced castings was influenced by the copper additions.

Microstructure

SEM micrograph of the unalloyed grey cast iron sample is depicted in Plate 1. Plates 2-4 are SEM micrographs of 1.4%wt Cu alloyed, 1.8%wt Cu alloyed, and 2.2%wt Cu alloyed grey cast iron samples respectively. Generally, the microstructure of the unalloyed grey cast iron sample is comprised of spatially dispersed elongated graphite flakes in ferrite matrix. While the microstructures of the copper alloyed samples are characterized by different graphite morphologies in multiphase matrix of pearlite and/or ferrite. The elongated graphite flakes in ferrite matrix of the unalloyed grey cast iron sample may be attributed to minimum undercooling that resulted during solidification of the melt (Stan et al., 2010).

Copper addition to grey cast iron promotes graphitization, refines and stabilizes pearlite (Riposan et al., 2012; Stan et al., 2010). Therefore, the differently featured morphology of graphite flakes in ferrite-pearlite matrix of the 1.4%wt Cu alloyed, 1.8%wt Cu alloyed, and 2.2%wt Cu alloyed grey cast iron samples may be due to effects of copper addition (Riposan et al., 2012). Also, the different undercooling conditions (high, moderate and low), which could have resulted from varying percent copper addition, may be contributory (Riposan et al., 2012).

Corrosion behaviour

From Plates 1-4, it can be deduced that localized corrosion is the primary type of degradation of the unalloyed and alloyed samples in 0.5 M HCl and 0.5M NaCl solutions (Maker & Tromans, 1995; Shtanko, 1980). The shifts towards less positive potential of the unalloyed sample relative to the alloyed samples in both 0.5 M HCl and 0.5M NaCl solution as shown by the polarization curves in Figure 2 and Figure 4 respectively are indications that the former is more anodic that the latter, and hence, the corrosion resistance of the unalloyed sample is poor relative to the alloyed sample in both the acid and salt environments. Characteristically, copper is resistant to corrosion (Krivosheev et al., 1973). Therefore, the high corrosion resistance of the alloyed samples is attributable to the effect of copper. In addition, the refinement and stabilization of pearlite phase that resulted from copper additions could have as well contributed (Krivosheev et al., 1973; Lunarska, 1996). Past research findings have shown that pearlite and ferrite phases corrode more readily as compared to graphite phase (Mohebbi & Li, 2011; Ruscak & Perng, 1995; Tel'manova et al., 1980). It can therefore be submitted that high rate of corrosion rate of the unalloyed sample relative to the alloyed samples in 0.5 M HCl (Figure 3) and 0.5M NaCl (Figure 5) was influenced by the different phases. Increasing shifts towards less positive potential (more anodic), and hence, increasing corrosion kinetics of the copper alloyed grey cast iron samples in order of 1.8%wt. Cu, 1.4%wt. Cu and 2.2%wt. Cu additions, may be due to the microstructural modification. Pearlite has shown poor capacity to passivate relative to ferrite (Ujiro et al., 1994). Therefore, low corrosion resistance of the 2.2wt. % Cu alloyed grey cast iron samples may have resulted from the presence of more volume fraction of pearlite in the matrix. Other contributors included increased carbide-rich phase and rosette morphology.

CONCLUSIONS

Based on the results of the investigation, the following conclusions were drawn:

i. The microstructure of the unalloyed casting is characterized by spatially dispersed elongated graphite flakes in ferrite-pearlite matrix. While the microstructures of the alloyed castings are characterized by different graphite morphologies in multiphase matrix of ferrite-pearlite.
ii. The corrosion behaviour of the both unalloyed and alloyed samples are influenced by the

microstructures, and the localized corrosion is the primary form of corrosion of all the castings.

iii. The unalloyed and copper alloyed samples revealed similar trend of corrosion behaviour in 0.5 M HCl and 0.5M NaCl solutions. However, the corrosion resistance of the unalloyed sample is poor relative to the alloyed sample in both the acid and salt environments.

iv. The highest and lowest corrosion behaviour in 0.5 M HCl and 0.5M NaCl solutions was shown by the 1.8wt%Cu alloyed and 2.2wt%Cu alloyed samples respectively.

REFERENCES

Adedayo, A.V. (2013). Relationship between graphite flake sizes and the mechanical properties of grey iron. *International Journal of Materials Science and Application, 2*(3), 94-98.

Agunsoye, J. O., Bello, S. A., Hassan, S. B., Adeyemo, R. G., & Odii, J. M. (2014), The effect of copper addition on the mechanical and wear properties of grey cast iron. *Journal of Minerals and Materials Characterization and Engineering,2,* 470-483.

American Society of Testing Materials, ASTM A247. (2006). *Standard test method for evaluating the microstructure of graphite in iron castings.* ASTM International, 100 Barr Harbor Drive, West Conshohocken, PA 19428 2959 USA.

Collini, L., Nicoletto, G., & Konecna, R. (2008). Microstructure and mechanical properties of pearlitic grey cast iron. *Materials Science and Engineering*, A *488*(1-2), 529–539.

Davis, J. R. (1996). Classification and Basic Metallurgy of Cast Irons. *American Society of Metal (ASM), Specialty Handbook Cast Irons,* 10-20. doi: 10.11648/j.ijmsa.20130203.14x

Hammood, S., & Ali, L. M. H. (2012). Development artificial neural network model to study the influence of oxidation Process and zinc-electroplating on fatigue life of gray cast iron. *International Journal of Mechanical and Mechatronics Engineering, 12* (5),74 – 78.

Krause, D. E. (1969). Gray iron—A unique engineering material. In H. Heine (Ed.), *Gray, Ductile, and Malleable Iron Castings—Current Capabilities.* West Conshohocken, Pennsylvania A: ASTM International

Krivosheev, A.E., Marinchenko, B. V., & Fetisov, N. M. (1973). Corrosion resistance of cast iron with and without additive treatment. *Russ Cast Prod,3,* 86–87.

Lunarska, E. (1996). Effect of graphite shape on the corrosion of grey cast iron in phosphoric acid. *Journal of Materials and Corrosion,47*(10), 539 – 544.

Makar, G. L., & Tromans, D. (1995). Pitting corrosion of iron in weakly alkaline chloride solutions. *Corrosion Science*, *52*(4), 250–261.

Mohebbi, H., & Li, C. Q. (2011). Experimental investigation on corrosion of cast iron pipes. *International Journal of Corrosion*, http://dx.doi.org/10.1155/2011/506501

Pluphrach, G. (2010). Study of the effect of solidification on graphite flakes microstructure and mechanical properties of an ASTM a-48 grey cast iron using steel molds. *Songklanakarin Journal of Science and Technology, 32*(6), 613-618.

Riposan, I., Chisamera, M., Stan, S., & Barstow, M. (2012): Improving chill control in iron powder treated slightly hypereutectic grey cast iron. *China Foundry*,8(2), 228 - 229.

Ruscak, M., & Perng, T. P. (1995). Effect of ferrite on corrosion of Fe-Mn-Al alloys in sodium chloride solution. *Corrosion Science*, *51*(10), 738 - 743.

Seidu, S. O. (2014). Effect of compositional changes on the mechanical behavior of grey cast iron. *Journal of Metallurgical Engineering*,3(2), 231- 239.

Sherrif, O. S., Saliu, O. S., Taiwo, S.A., &. Lulian, R. (2019). Chilling effect of iron powder on the microstructure and hardness property of strongly hypereutectic grey cast iron. *ANNALS of Faculty Engineering Hunedoara- International Journal of Engineering, 4*, 13-22.

Stan, S., Chisamera, M., Riposan, I., Stefan, E., & Barstow, M. (2010). Solidification pattern of un-inoculated and inoculated gray cast irons in wedge test samples. *Transactions of the American Foundry Association* (AFS), 118, 295-309.

Tel'manova, O. N., Karyazin, P. P., & Shtanko, V. M. (1980). Behavior of cast-iron with lamellar and globular graphite in dilute acids. *Protection of Metals,16*(1), 45-47.

Ujiro, T., Yoshioka, K., & Staehle, R. W. (1994). Differences in corrosion behavior of ferritic and austenitic stainless-steels. *Corrosion Science*, 50(12), 33-4

Table 1: Chemical composition of the grey cast iron scrap

Element	C	Fe	Si	Cu	S	Ni	Mn	Al	Mo	P
Comp. (wt. %)	2.757	92.300	1.803	0.610	0.030	0.023	0.600	0.738	0.040	<0.100

Table 2: Chemical composition of the grey cast iron scrap

Grey Cast Iron	Chemical Composition wt.%						CE (wt. %)	Mn/ S	(Mn)x S
	C	Si	Mn	P	S	Al			
U.I.	3.08	2.45	0.234	0.088	0.135	0.0010	3.15	1.73	0.032
1.4wt.% Cu alloy	3.01	2.93	0.220	0.069	0.143	0.0076	3.08	1.54	0.031
1.8wt.%Cu alloy	3.10	2.98	0.201	0.060	0.140	0.0087	3.17	1.43	0.028
2.2wt.%Cu alloy	3.03	2.98	0.101	0.071	0.149	0.0098	3.10	0.68	0.015

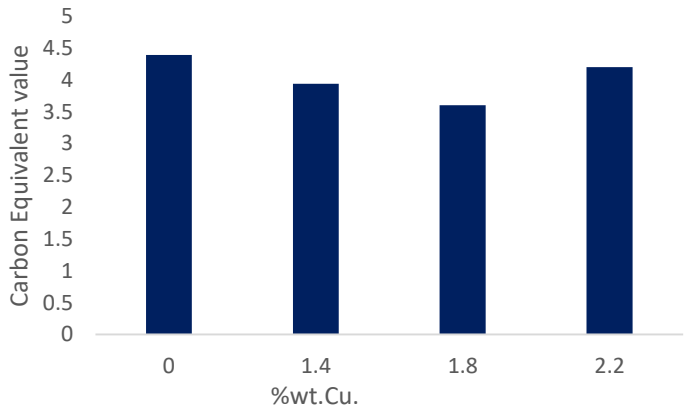

Figure 1. Effects of copper additions on carbon equivalent (CE) of the samples

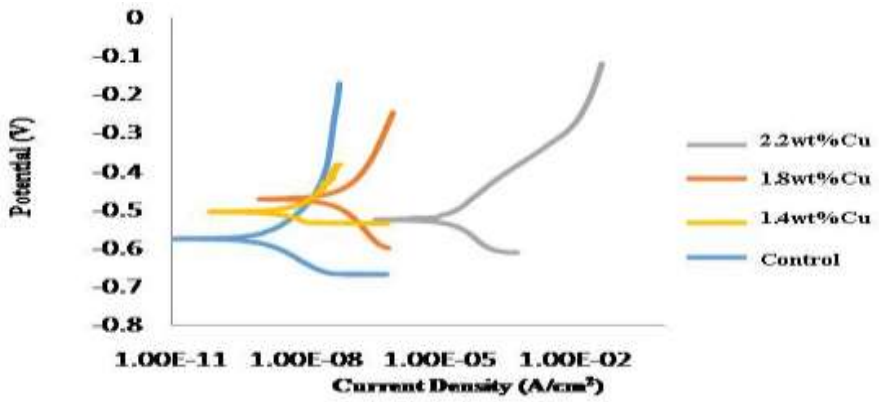

Figure 2. Potentiodynamic polarization curves of the unalloyed and alloyed samples in HCl

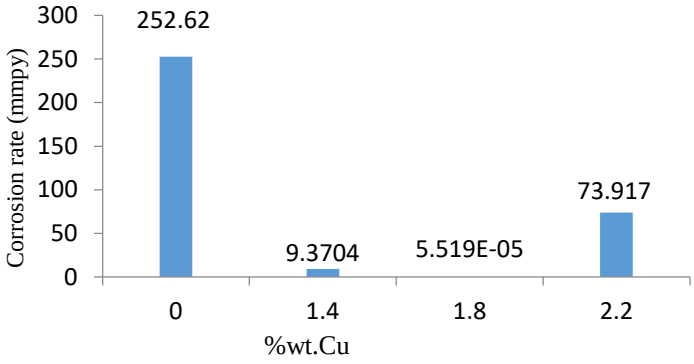

Figure 3. Corrosion rate of the unalloyed and alloyed samples in HCl environment

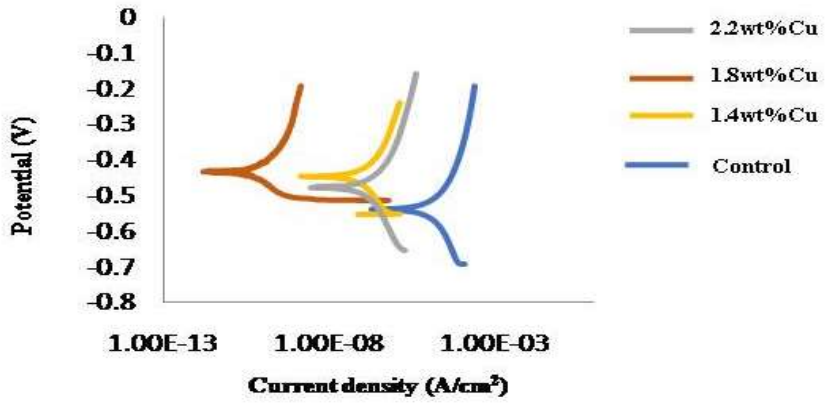

Figure 4. Potentiodynamic polarization curves of the unalloyed and alloyed samples in NaCl environment.

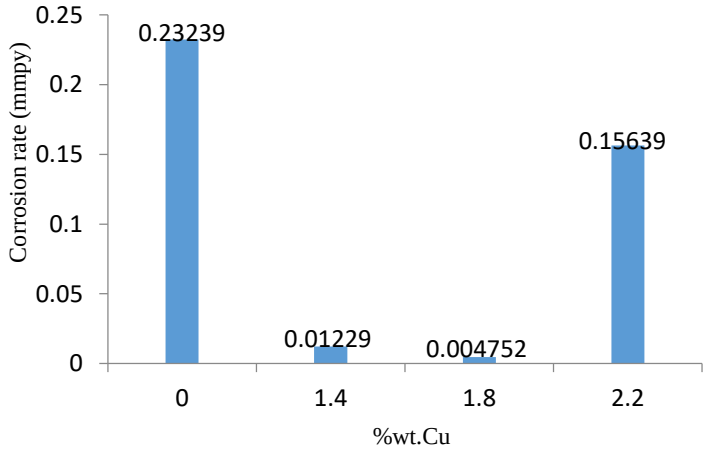

Figure 5. Corrosion rate of the unalloyed and alloyed samples in NaCl environment.

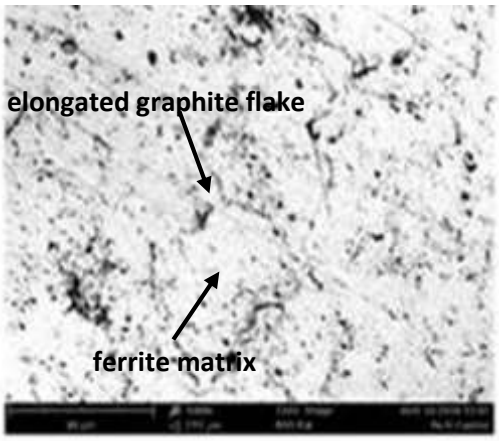

Plate 1. SEM micrographs of the unalloyed grey cast iron at mg. 1000x

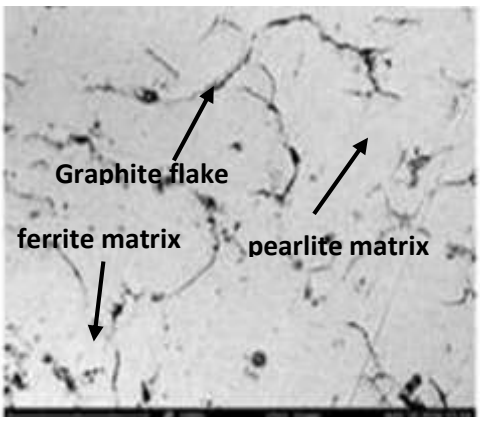

Plate 2. SEM micrographs of the 1.4wt%Cu copper alloyed grey cast iron at mg. 1000x

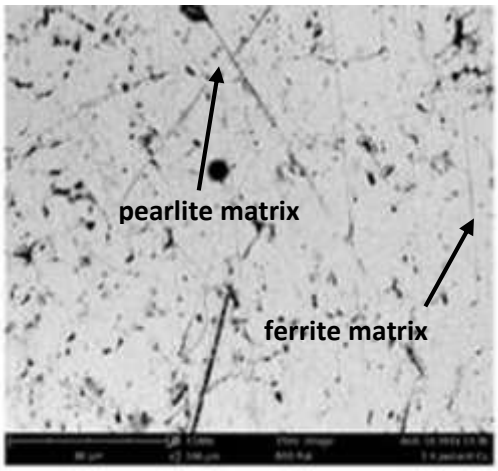

Plate 3. SEM micrographs of the 1.8wt. %Cu copper alloyed grey cast iron at mg. 1000x

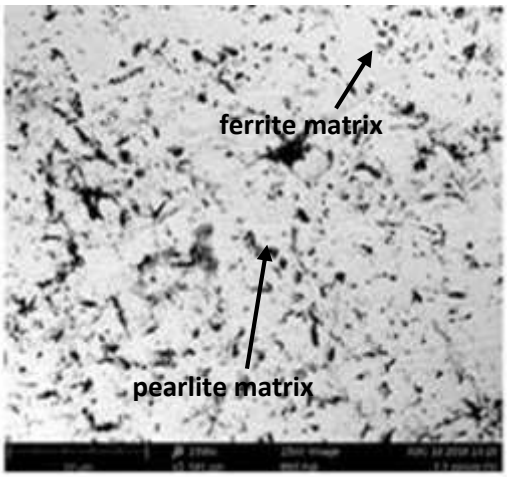

Plate 4. SEM micrographs of the 2.2wt. %Cu copper alloyed grey cast iron at mg. 1000x